NEW PETROLOGY, MINERAL CHEMISTRY AND STABLE MG ISOTOPE COMPOSITIONS OF AN ALLENDE CAI: EK-459-7-2. C. R. Jeffcoat[1], A. G. Kerekgyarto[1], T. J. Lapen[1], M. Righter[1], J. I. Simon[2], and D. K. Ross[3], [1]Department of Earth and Atmospheric Sciences, University of Houston, 312 Science and Research, Houston, TX, 77204 (crjeffcoat@uh.edu), [2]Center for Isotope Cosmochemistry & Geochronology, Astromaterials Research and Exploration Science Division, NASA-Johnson Space Center, Houston, TX, USA, [3]Jacobs Tech/NASA-JSC, Houston, TX 77058.

Introduction: Calcium–aluminum-rich inclusions (CAIs) are the key to understanding physical and chemical conditions in the nascent solar nebula. These inclusions have the oldest radiometric ages of solar system materials [1] and are composed of phases that are predicted to condense early from a gas of solar composition [2]. Thus, their chemistry and textures record conditions and processes in the earliest stages of development of the solar nebula.

Type B inclusions are typically larger and more coarse grained than other types with substantial evidence that many of them were at least partially molten. Type B inclusions are further subdivided into Type B1 (possess thick melilite mantle) and Type B2 (lack melilite mantle). Despite being extensively studied, the origin of the melilite mantles of Type B1 inclusions remains uncertain.

We present petrologic and chemical data for a Type B inclusion, EK-459-7-2, that bears features found in both Type B1 and B2 inclusions and likely represents an intermediate between the two types. Detailed studies of more of these intermediate objects may help to constrain models for Type B1 rim formation.

Methods: A polished plug of EK-459-7-2 was analyzed optically. X-ray elemental maps were collected on the NASA-JSC JEOL 7600F with beam conditions of 15 kV and 30 nA at 130X magnification. Major and minor element abundances were determined on the NASA-JSC JEOL 8530F electron microprobe with beam conditions of 15 kV and 30 nA with a spot size of ~1 µm.

Laser ablation analyses for elemental abundances and Mg isotopes were collected at the University of Houston with a spot size of ~50 µm and a pulse rate of 10 Hz. Elemental abundances of phases in EK-459-7-2 plug were analyzed with a Varian 810 inductively coupled plasma mass spectrometer coupled with a Photon Machines Analyte 193 eximer laser-ablation system (LA-ICP-MS). Al-Mg isotope compositions were collected on a NuPlasma II multicollector inductively coupled plasma spectrometer coupled with a Photon Machines Analyte 193 eximer laser-ablation system (LA-MC-ICP-MS).

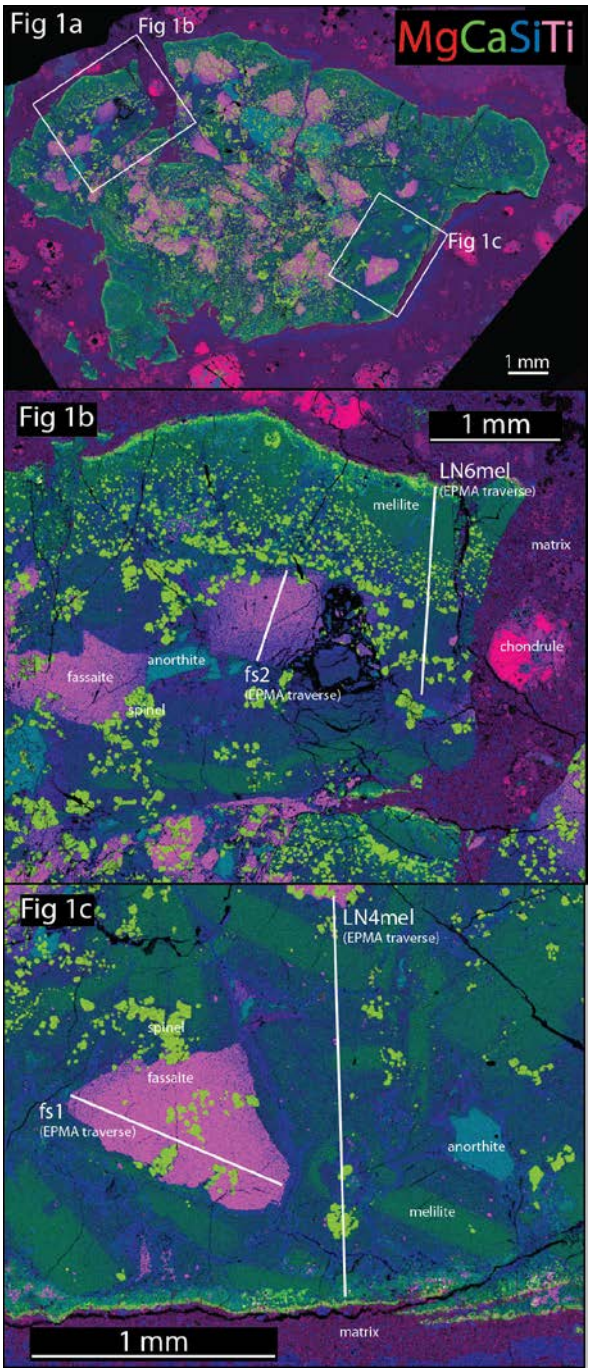

Figure 1: Composite X-ray element maps. a) whole inclusion, b) Type B1-like portion of the inclusion, c) Type B2-like portions of the inclusion.

Results and Discussion:

Modal abundances and bulk composition. The modal abundances of the primary phases were estimated using image analysis software and are: melilite (~50%), fassaite (~17%), anorthite (~12%), spinel (~21%). Bulk composition for EK-459-7-2 plots well within the field of typical Type B CAIs and very near the calculated compositions that represent ~40% Mg loss from a condensate from a gas of solar composition [3]. SiO_2 bulk composition (~25 wt. % SiO_2) is moderately low for Type B CAIs.

The coarse grain size and interlocking texture are strong evidence that this object was melted, or at least partially melted, during its history. Based upon textural relationship of the phases and the bulk chemical composition (i.e. theoretical and experimentally determined phase relationships; e.g. [4]) spinel and melilite were likely the first phases to form followed by anorthite and fassaite later. The presence of large anorthite, moderate to low SiO2 bulk compositions, and lack of reverse zoning in melilite suggests that anorthite began to crystallize before fassaite; however, the large size and subhedral shape of the fassaite indicate some fassaite began crystallizing shortly after anorthite if not at the same time.

Textures and mineral chemistrty. EK-459-7-2 has textural and mineralogical characteristics found in both Type B1 and Type B2 CAIs (Fig. 1a). On one portion of the CAI margin (Fig. 1b), a distinct melilite mantle (~1 mm thick) is present. The melilite mantle in this area is composed of radial laths extending from the exterior rim toward the interior and the Åk content of the melilite ranges from ~Åk15 near the margin up to ~Åk65 toward the interior. The margin of much of the CAI possesses this B1-like character. Small (<50 μm diameter) spinel are abundant in the B1-like regions; however, the amount of spinel in the mantle decreases with an increase in B1-like mantle character. Fassaites that grow adjacent to the interior edge of the melilite mantle commonly display compositional zoning radially from the mantle edge inward and are more Ti-poor (TiO2 = 1.7-8.6 wt%; all Ti reported as TiO2) than those in the B2 portions. Melilite in the interior but near the melilite mantle displays very little compositional zoning and is more Åk-rich than the adjacent mantle melilite.

Fig. 1c shows the portion of the mantle with a B2 character. The melilite laths in this portion of the margin are more randomly oriented but most grains do contact the WL-rim at a similar oblique angle. Melilites in this region are compositionally zoned with uniformly Åk-poor (~Åk10-15) cores to more Åk-rich (~Åk30-40) rims that transitions over a only a few micrometers. This portion of the margin contains fassaite that show no preferred orientation in compositional zoning and are more Ti-rich (TiO2 = 1.6-13.4 wt%; all Ti reported as TiO2) than the B1 area.

REE compositions for the CAI phases measured were normalized to the values of [5]. REE abundances for fassaite increase with atomic number with large negative Eu-anomalies. The melilites in general have flat REE patterns and Eu-anomalies that are generally either absent or positive. The anorthite REE abundances are very low for the HREE, show an increase with a decrease in atomic number, and large positive Eu-anomalies. Total REE abundances in general are higher at the egdes of all phases and can be modeled by fractional crystallization.

Stable Mg isotopes. Stable Mg isotope variations in δ^{25}Mg from CAI margin and core were conducted. The interior of the object is uniformly enriched in heavy isotopes with δ^{25}Mg ~11.5 ‰. δ^{25}Mg decreases toward the CAI margin to δ^{25}Mg ~4 ‰ near the edge of the object for both the B1- and B2-like regions. However, the decrease occurs sharply in the B2-like margin over <200μm near the margin and gradually over >800μm for the B1-like melilite mantle.

Brittle fracturing and fragmenting. EK-459-7-2 is a highly fragmented object, but most fragments have stayed juxtaposed to one another providing continuity across most of the smaller cracks. There does exist continuity between portions of the object that display both B1 and B2 characteristics. Many cracks within the CAI terminate at the CAI boundary and do not continue into the matrix. Additionally, fragment boundaries that protrude into the matrix do not appear to disturb the matrix material in any way.

The fracturing and fragmentation of EK-459-7-2 suggests deformation prior to parent body accretion. Likewise, the brittle edge of adjacent fragments do not show any continuation or disturbance of matrix indicating that the fracturing occurred before dust accretion or before consolidation of accreted dust that surrounds the matrix.

References: [1] Bouvier, A. and Wadhwa, B. (2010) Nature, 3, 637-641. [2] Grossman, L. (1972) GCA, 36, 597-619. [3] Grossman, L. et al. (2000) GCA, 64, 2879-2894. [4] Stolper, E. and Paque, J.M. (1986) GCA, 50, 1785-1806. [5] Dauphas, N. and Pourmand, A. (2015) GCA, 163, 234-261